Numerical Simulation of Ash Vaporization during Pulverized Coal Combustion in the Laboratory-Scale Single-Burner Furnace

ARTICLE *in* ENERGY & FUELS · APRIL 2005

Impact Factor: 2.79 · DOI: 10.1021/ef049693l

7 AUTHORS, INCLUDING:

Yu Qiao
Huazhong University of Science and Technol…
32 PUBLICATIONS **461** CITATIONS
SEE PROFILE

Yun Yu
Curtin University
44 PUBLICATIONS **795** CITATIONS
SEE PROFILE

Xiaowei Liu
Harbin Institute of Technology
213 PUBLICATIONS **916** CITATIONS
SEE PROFILE

Xiangpeng Gao
Curtin University
30 PUBLICATIONS **318** CITATIONS
SEE PROFILE

Numerical Simulation of Ash Vaporization during Pulverized Coal Combustion in the Laboratory-Scale Single-Burner Furnace

Jiancai Sui, Minghou Xu,* Jihua Qiu, Yu Qiao, Yun Yu, Xiaowei Liu, and Xiangpeng Gao

State Key Laboratory of Coal Combustion, Huazhong University of Science and Technology, Wuhan 430074, China

Received November 29, 2004. Revised Manuscript Received March 4, 2005

CFD tools have been developed to effectively simulate complex, reacting, multiphase flows that exist in utility boilers. In this paper, a model of ash vaporization was established and integrated into a self-developed CFD code to predict ash vaporization in the coal combustion process. Experimental data from a single-particle combustion was used to validate the above model. The calibrated model was then applied to simulate the ash vaporization in a 92.9 kW laboratory-scale single-burner furnace. The effects of different combustion conditions, including air staging, on the ash vaporization were investigated. The results showed that the fraction of ash vaporization is mostly sensitive to coal particle temperature. Ash vaporization primarily occurred after a short interval along the coal particle trajectories when the particle temperatures increased to 1800 K. Air staging influenced the ash vaporization by changing the gas temperature distribution in the furnace. The simulation results showed that the more extreme the staging condition, the lower the overall peak temperature, and hence the lower the amount of ash vaporization.

1. Introduction

Particulate matter (PM) generated by coal combustion has become an increasingly important environmental concern due to its adverse environmental and health effects in China. The amount of PM emission from coal-fired plants with a capacity of 6 MW was 3.97 Mt, accounting for 28% of the national total of 14.14 Mt in 1996.[1] Moreover, due to the low thermal efficiency of coal-fired boilers and the prevalence of low rank coal in China, PM emission from coal combustion accounts for about 1.2−1.5% of the consumed coal in the power generation plant, causing the most severe environmental pollution.[2] In the absence of control techniques, the annual average PM concentration in all Chinese cities was 432 mg/m^3 in 1989, which is far higher than the limit value, ranging from 15 to 50 mg/m^3 in the developed countries.[1,3,4]

Field studies[5−7] and laboratory investigators[8,9] find that the combustion-generated ash particles are bimodally distributed with respect to particle size. The larger particles, which will be termed coarse particulate, are formed by included mineral coalescence, char, and excluded mineral fragmentation. The smaller ash particles, which will be termed fine particulate or submicrometer (1 μm or less), are formed by vaporization and subsequent condensation of mineral matter. The fine particles are particularly troublesome because they are the ones most likely not to be captured completely in pollution abatement equipment.[10−12] Therefore, several investigators have studied the formation of coal combustion-derived fine particulate and its affecting factors.

Early studies of the effect of combustion conditions on submicrometer ash formation included the work of

* Corresponding author. Tel.: +86-27-8754-4779. Fax: +86-27-8754-5526. E-mail: mhxu@mail.hust.edu.cn.

(1) Soud, H. N.; Wu, Z. *East Asia-air Pollutant Control and Coal-Fired Power Generation*; IEA Coal Research: London, U.K., June 1998.

(2) Tao, S.; Ma, Y. The environmental monitoring in thermal power plant in China. In *Proceedings of International Conference on Environmental Protection of Electric Power*, Nanjing, China, 1996; pp 65−73.

(3) Aerosol from Biomass Combustion, the International Seminar at 27 June 2001 in Zurich by IEA Bioenergy task 32; Thomas, N., Ed.; Biomass Combustion and Cofiring and Swiss Federal Office of Energy: Verenum, Zurich, 2001.

(4) Yoshihiko, N.; Lian, Z.; Atsushi, S.; Zhongbing, D. Influence of coal particle size on particulate matter emission and its chemical species produced during coal combustion. *Fuel Process. Technol*. **2004**, *85*, 1065−1088.

(5) Markowski, G. R.; Ensor, D. S.; Hooper, R. G.; Carr, R. C. A submicron aerosol mode in flue gas from a pulverized coal utility boiler. *Environ. Sci. Technol.* **1980**, *14*, 1400−1402.

(6) Ylatalo, S. I.; Hautanen, J. *Aerosol Sci. Technol.* **1998**, *29*, 17−30.

(7) McElroy, M. W.; Carr, R. C.; Ensor, D. S.; Markowski, G. R. Size distribution of fine particles from coal combustion. *Science* **1981**, *215*, 13−19.

(8) Mulholland, J. A.; Sarofim, A. F.; Guangxi, Y. The transformation of inorganic particles during suspension heating of simulated wastes. *Environ. Prog.* **1991**, *10* (2), 84−89.

(9) Quann, R. J.; Sarofim, A. F. Vaporization of refractory oxides during pulverized coal combustion. In *Nineteenth Symposium (international) on Combustion*; The Combustion Institute: Pittsburgh, PA, 1982; pp 1429−1440.

(10) Germani, M. S.; Zoller, W. H. Vapor-phase concentrations of arsenic, selenium, bromine, iodine and mercury in the stack of a coal-fired power plant. *Environ. Sci. Technol.* **1988**, *22*, 1079−1085.

(11) Shendrikar, A. D.; Ensor, D. S.; Cowen, S. J.; Woffinden, G. J. Size-dependent penetration of elements through a utility baghouse. *Atmos. Environ.* **1983**, *17*, 1411.

(12) Kauppinen, E. I.; Pakkanen, T. A. Coal combustion aerosols: A field study. *Environ. Sci. Technol.* **1990**, *24*, 1811−1818.

10.1021/ef049693l CCC: $30.25
Published on Web 04/22/2005

Schmidt and co-workers,[13] which proved inconclusive, and the later pilot-scale studies by Flagan and Taylor,[14] which showed that submicrometer ash formation increased with increasing combustion intensity. This observation is consistent with the expectation that ash vaporization increases with increasing combustion temperature. Later studies showed the effect of combustion temperature[9,15] and air staging[16] on ash vaporization. The increase in ash vaporization with increasing temperature is clear. The impact of staged combustion on ash vaporization is less clear. In a staged combustor, the coal particles encounter lower temperatures and spend more time under reducing conditions. The reducing environment could conceivably counteract the lower temperatures and promote the ash vaporization. The mixed results on the effect of staging on ash vaporization observed by Linak and Peterson[16] may be a result of the possible trade-off between temperature and reducing conditions as the combustor is staged. Since only a few studies are to be found in the literature devoted to the effect of staging on ash vaporization, the trade-off needs to be evaluated by field and laboratory testing or by CFD modeling. Unfortunately, up to now, there are very few groups who have calculated the vaporization of ash by CFD modeling. Only Lockwood and co-workers[17,18] have addressed the detailed temperature and residence-time distribution in a combustor using a CFD code. They set up the aerosol dynamics equations, allowing for the nucleation and condensation of vapor species and for the coagulation of the aerosols. However, the scope of the effort was limited by assuming that either 2.4%[17] or 3%[18] of the total ash is in the submicrometer fraction, rather than calculating it on the basis of the actual conditions.

On the basis of the above considerations, this paper simulates the ash vaporization during coal combustion by using a self-developed CFD code and aims to study the influences of air staging on ash vaporization. As the refractory oxides of Al, Ca, Fe, Mg, and Si account for most of the submicrometer particles, the amount of ash vaporization can be calculated by summing the amount of refractory oxide vaporization. In this work, a model for simulating the ash vaporization (that is, refractory oxide vaporization) during coal combustion is developed and integrated with the self-developed CFD code. The behavior of ash vaporization under different combustion conditions, including air staging, in a 92.5 kW laboratory-scale single-burner furnace is then simulated.

2. Transformation of Mineral Matter during Combustion

For Chinese coals, approximately 20% (wt) of coal fired is present as mineral constituents and other inorganic compounds. The most common mineral forms, which incorporate the major inorganic elements in coal, include quartz, alumino-silicate clays, calcite, siderite, and pyrite. At flame temperature in combustion (1700−2500 K), the minerals will decompose rapidly and melt, yielding molten metal oxide droplets. As the char surface recedes during heterogeneous combustion, the molten inclusions will tend to adhere to the char's surface and, to a certain extent during the latter stages of char burnout, coalesce or contact to form larger ash droplets. Particulates generated by this process will range in size from about 1 μm to much larger sizes but typically averaging about 10 μm.[19] Not all of the ash is necessarily released in this manner. At flame temperature, it is expected that a number of relatively volatile trace metals in coal will volatilize completely. When coal particles burn at high temperatures (above 1800 K), the carbon oxidation rate is sufficiently fast that oxygen partial pressures within the porous char are extremely low. Under these conditions, the locally reducing environment occurring within the burning char particles may facilitate the chemical reduction of refractory metal oxides to highly volatile suboxides (SiO, Al_2O) or metals (Mg, Ca, and Fe). As suboxides or metal vapors diffuse out of the char and through the char external boundary layer, they encounter increasing oxygen potential of the bulk gas. Reoxidation or combustion of metal vapors in the gas phase results in supersaturation with respect to the oxide vapors thus formed and subsequent condensation by homogeneous nucleation of extremely fine particles of metal oxides. The fine particles of the metal oxide fume will then grow by collision and coagulation processes to mean diameters in the range of 0.1 to 0.5 μm.[19,20] A bimodal distribution of ash is the consequence of the two particulate formation mechanisms. The schematic of the processes that govern the formation of ash particles during combustion is shown in Figure 1.[21]

3. Ash Vaporization Model

The vaporization of suboxides or metals can be modeled assuming that the reduction of the refractory oxides by CO occurs via heterogeneous reaction

$$MO_n(s) + CO \rightarrow MO_{n-1}(g) + CO_2 \qquad (1)$$

where MO_n and MO_{n-1} refer to the refractory oxide and the corresponding volatile suboxide (SiO, Al_2O) or metal (Mg, Ca, and Fe) vapor, respectively. This reaction is further assumed to be at equilibrium at the surface of each inclusion within the char particle. The partial pressure of the metal or suboxide vapor P^i_m at an

(13) Schmidt, E. W.; Gieseke, J. A.; Allen, J. M. *Atmos. Environ.* **1976**, *10*, 1065.
(14) Taylor, D. D.; Flagan, R. C. *Aerosol Sci. Technol.* **1982**, *1*, 103−117.
(15) Mims, C. A.; Neville, M.; Quann, R. J.; House, K.; Sarofim, A. F. *AIChE Symp. Ser.* **1980**, *76* (201), 188−194.
(16) Linak, W. P.; Peterson, T. W. Mechanisms governing the composition and size distribution of ash aerosol in a laboratory pulverized coal combustor. In *Twenty-First Symposium (International) on Combustion*; The Combustion Institute: Pittsburgh, 1986; pp 399−410.
(17) Abbas, T., Costen, P., De Soete, G., Glaser, K., Hassan, S., Lockwood, F. C., Eds. *Twenty-Sixth Symposium (International) on Combustion*; The Combustion Institute: Pittsburgh, PA, 1996; pp 2487−2493.
(18) Yousif, S.; Lockwood, F. C.; Abbas, T. Modeling of toxic metal emissions from solid fuel combustors. In *Twenty-Seventh Symposium (International) on Combustion*; The Combustion Institute: Pittsburgh, PA, 1998; pp 1647−1654.
(19) Quann, R. J.; Neville, M.; Janghorbant, M.; Mims, C. A.; Sarofim, A. F. Mineral Matter and Trace-Element Vaporization in a Laboratory Pulverized Coal Combustion System. *Environ. Sci. Technol.* **1982**, *16* (16), 776−781.
(20) Desrosiers, R. S.; Riehl, J. W.; Ulrich, G. D.; Chiu, A. S. In *Seventeenth Symposium (International) on Combustion*; The Combustion Institute: Pittsburgh, PA, 1979; pp 1395−1406.
(21) Lockwood, F. C.; Yousif, S. A model for the particulate matter enrichment with toxic metals in solid fuel flames. *Fuel Process. Technol.* **2000**, 65−66, 439−457.

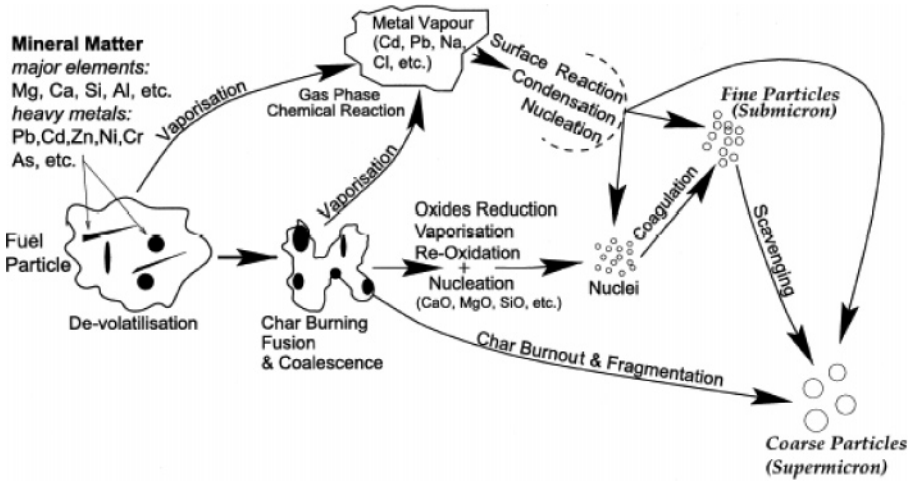

Figure 1. Schematic of mineral transformation during coal combustion.

inclusion surface is therefore given by

$$P^i_{\mathrm{m}} = K_i \frac{\alpha_m P_{\mathrm{CO}}}{P_{\mathrm{CO_2}}} \tag{2}$$

where K_i is an equilibrium constant, the value of which can be obtained by fitting the data in the JANAF tables;[22] $P_{\mathrm{CO_2}}$ and P_{CO} are the local partial pressures of CO_2 and CO, respectively; α_{m} is the activity of the solid metal oxide, the value of which is assumed to be 1. The Krishnamoorthy[23] result is used to calculate the $P_{\mathrm{CO}}/P_{\mathrm{CO_2}}$ ratio in this paper, the expression for which is

$$\frac{P_{\mathrm{CO}}}{P_{\mathrm{CO_2}}} = K \exp\left(\frac{A}{T_{\mathrm{ref}}} - \frac{A}{T}\right) \exp[B(P_{\mathrm{CO_2,ref}} - P_{\mathrm{CO_2}})]\left(\frac{d_{\mathrm{p,ref}}}{d_{\mathrm{p}}}\right)^C \tag{3}$$

The coefficients of eq 3 can be obtained from ref 23, but it should be noticed that the coefficients A and B are switched in this document.

The total vaporization rate of individual metal oxides from a single char particle is calculated by using Quann and Sarofim's model;[9] the model result is

$$V_{\mathrm{c}} = \eta N_I 4\pi r_m D_{\mathrm{e}} c X^i_{\mathrm{m}} \ (\mathrm{mol/s}) \tag{4}$$

where

$$\eta = \frac{3}{\Phi}\left[\frac{1}{\tanh \Phi} - \frac{1}{\Phi}\right]\left[1 + \frac{D_{\mathrm{e}}}{\alpha D_{\mathrm{O}}}\left(\frac{\Phi}{\tanh \Phi} - 1\right)\right]^{-1}$$

$$\Phi = (3\theta)^{1/2}\frac{r_0}{r_m}$$

$$\alpha = \left[1 - \exp\left\{-\frac{D_{\mathrm{O}}}{D_{\mathrm{m}}}\ln(1 + x^b_{\mathrm{O}})\right\}\right]^{-1} \ln(1 + x^b_{\mathrm{O}})$$

where D_{e} is the effective Knudsen diffusivity; D_{O}, oxygen diffusivity in bulk gas; D_m, diffusivity of element or suboxide in bulk gas; x^b_{O}, mole fraction of O_2 in bulk gas; $N_I = \theta(r_0/r_m)^3$, number of inclusions in the char particle; θ, volume fraction of the inclusion; r_0, char particle radius; r_m, inclusion radius; X^i_{m}, mole fraction of vapor at inclusion surface; c, concentration of gas.

Because $cX^i_{\mathrm{m}} = P^i_{\mathrm{m}}/(RT)$, one can obtain

$$V_{\mathrm{c}} = \eta N_I 4\pi r_m D_{\mathrm{e}} \frac{P^i_{\mathrm{m}}}{RT} \tag{5}$$

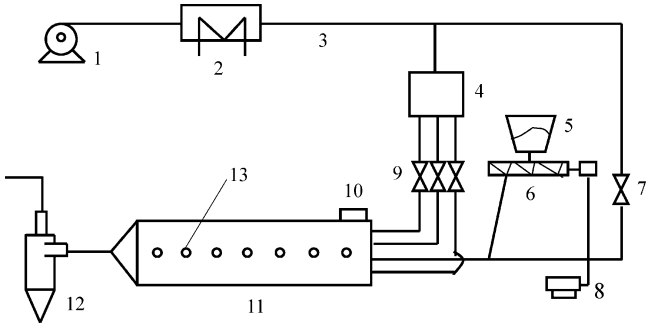

Figure 2. Schematic diagram of laboratory single-burner furnace. Legend: 1, blower; 2, air preheater; 3, air pipe; 4, secondary air distributor; 5, pulverized coal hopper; 6, pulverized coal feeder; 7, primary air valve; 8, electric motor; 9, secondary air valve; 10, observation window; 11, furnace; 12, cyclone separator; and 13, sampling points.

As mentioned previously, CFD tools have been developed that are capable of effectively simulating the complex, reacting, multiphase flows that exist in utility boilers. In the present work, the above vaporization model is integrated into a CFD code to simulate the ash vaporization process during combustion. Experimental data from a single-particle combustion process was used to validate and calibrate the vaporization. The code after minor modifications was then used to simulate ash vaporization in a laboratory-scale single-burner furnace.

4. Numerical Simulation

4.1. Laboratory-Scale Single-Burner Furnace. The laboratory-scale single-burner furnace simulated is schematically shown in Figure 2. The furnace is 4 m long and has a cross-section of 0.35 × 0.5 m. From the top to the bottom, the burners are arranged in the order of upper secondary air, middle secondary air, primary air, and lower secondary air, as shown in Figure 3. All the secondary air ports have the same cross-section of

(22) *JANAF Thermochemical Tables*, 2nd ed.; NSDRSNBS37, U.S. National Bureau of Standards, Gaithersburg, MD, 1971.

(23) Gautham, K.; Veranth, J. M. Computational modeling of CO/CO_2 ratio inside single char particles during pulverized coal combustion. *Energy Fuels* **2003**, *17*, 1367−1371.

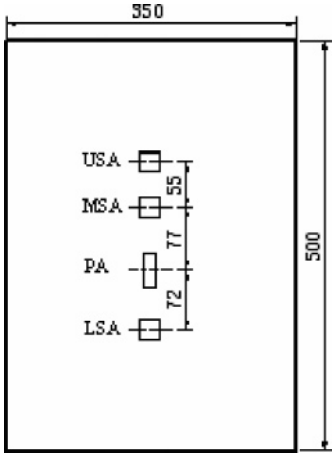

Figure 3. Schematic diagram of air ports arrangement (dimensions in millimeters).

24 mm × 24 mm, and the cross-section of primary air port is 14 mm × 42 mm.

4.2. Mathematical Models and Numerical Method. The mathematical models and numerical method employed in CFD code here have been described in detail elsewhere[24] and are as follows.

The gas flow is described by time-averaged conservation equations of mass, momentum, enthalpy, and species. The turbulence is treated by the $k-\epsilon$ two-equation model. The stochastic particle trajectory (SPT) model is used to simulate the two-phase flow of pulverized coal in the furnace. For simulation of radiation heat transfer, the discrete transfer method is used.

A finite volume differencing scheme solves the gas-phase transport equation of mass, momentum, enthalpy, gas species (mixture fraction), and equations of turbulence. The SIMPLER method of pressure correction is used. Coal combustion is modeled using the mixture fraction concept. Coal particles are tracked in Lagrangian procedure.

5. Results and Discussion

5.1. Simulation of the Vaporization of a Single Particle. To simulate and analyze the ash vaporization behavior in the laboratory-scale single-burner furnace, the ash vaporization of a single coal particle was first simulated. Furthermore, the results by the initial vaporization model were used to compare with experimental data, and thus to validate the model. Some of the experimental data for ash vaporization was obtained from ref 9 for 14 different coals. The distribution of temperature and gas concentration was simulated by the self-developed CFD code. The mineral inclusion size for 14 different coals applied Lee and Eddings' calculation results[25,26] after minor modifications. It can be found that the calculated vaporization fraction of oxides for Illinois No. 6 bituminous is consistent with the experimental data, as shown in Figure 4.

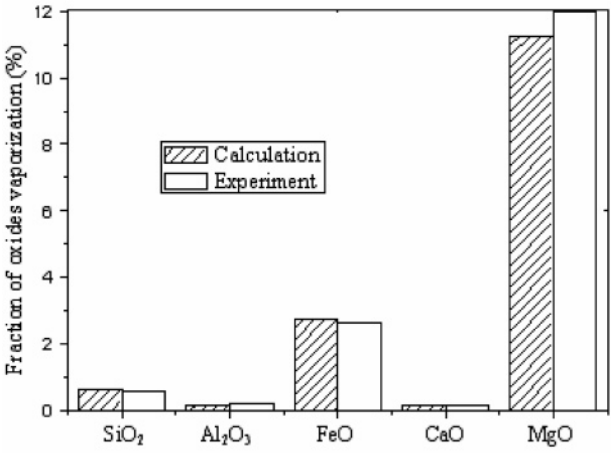

Figure 4. Predicted and measured[9] oxides vaporization of Illinois No. 6 bituminous: 60-μm-diameter particles burning in 20% oxygen at a furnace temperature of 1750 K.

5.2. Simulation of Vaporization in a Laboratory-Scale Single-Burner Furnace. The above single-particle calculation can be used to validate the vaporization model and obtain the inclusion sizes for each coal studied. Then, CFD simulations were performed for the single-burner furnace. Coal burned in this furnace has characteristics similar to those of Illinois No. 6 bituminous. Its inclusion sizes were used for the ash vaporization calculation in the furnace. The proximate analysis of this coal is shown in Table 1.

Air staging during pulverized coal combustion is a known means of controlling NO_x emission. However, the effect of air staging on ash vaporization is not quite clear. To investigate the influence of air staging on ash vaporization, several cases were simulated. As the size of the furnace is relatively small, changing the ratio of the primary air (PA) will result in poor combustion conditions in this furnace. Furthermore, the port of the lower secondary air (LSA) is located close to that of PA, and LSA has a function to hold the pulverized coal. Therefore, in this simulation, the ratio of PA and LSA to total airflow rate (TAR) was kept constant, and the intensity of staging was varied by changing the feeding rate of the middle secondary air (MSA) and upper secondary air (USA). The operating conditions of each computation case are listed in Table 2.

Figure 5 shows the gas temperature profiles for three cases in the centerline of the furnace half zone near the port outlet. Obvious differences occur for three cases, the position of the corresponding peak temperature moves sequentially toward the ports from case 1 to case 3. The peak temperature in three cases is 1717, 1908, and 1652 K, respectively. The probable causes of the variety of the peak temperature in three cases are that, with the MSA rate reduced gradually from case 1 to case 2, the mixing of pulverized coal with the secondary air is improved, and the pulverized coal is almost burnt out in these cases; however, the mixing of pulverized coal with the secondary air becomes bad for case 3. This has a great effect on the pulverized coal combustion and renders a decrease of the peak temperature. In other words, the model predictions showed that for the laboratory-scale furnace simulated here, the more extreme the staging condition is, the lower the overall peak temperature.

(24) Minghou, X.; Jianwei, Y.; Shifa, D.; Handing, C. Simulation of gas temperature deviation in large-scale tangential coal fired utility boilers. *Comput. Methods Appl. Mech. Eng.* **1998**, *155*, 369−380.

(25) Lee, C. M.; Davis, K. A.; Heap, M. P.; Eddings, E. G.; Sarofim, A. S. Modeling the vaporization of ash constituents in a coal-fired boiler. In *Twenty-Eighth International Symposium (International) on Combustion*; The Combustion Institute: Pittsburgh, PA, 2000; pp 2375−2382.

(26) Eddings, E. G.; Sarofim, A. F.; Lee, C. M.; Davis, K. A.; Valentine, J. R. Trends in predicting and controlling ash vaporization in coal-fired utility boilers. *Fuel Process. Technol.* **2001**, 71, 39−51.

Table 1. Proximate Analysis of Actual Coal

rank	H_2O (wt % as received)	ash (wt % as received)	volatile matter, VM (wt % as received)	fixed carbon, FC (wt % as received)	nitrogen, N (wt % as received)	low heating value, Q (kJ/kg)
B[a]	12	15	41.01	59.29	0.9	30901

[a] Bituminous.

Table 2. Computation Cases

case	ratio of MSA[a] (%)	ratio of USA[b] (%)	ratio of LSA[c] (%)	ratio of PA[d] (%)	TAR[e] (kg/ h)	fuel feed rate (kg/h)	air temperature (×bcC)
1	23	23	30	24	126.7	20	250
2	15.3	30.7	30	24	126.7	20	250
3	0	46	30	24	126.7	20	250

[a] Middle secondary air. [b] Upper secondary air. [c] Lower secondary air. [d] Primary air. [e] Total airflow rate.

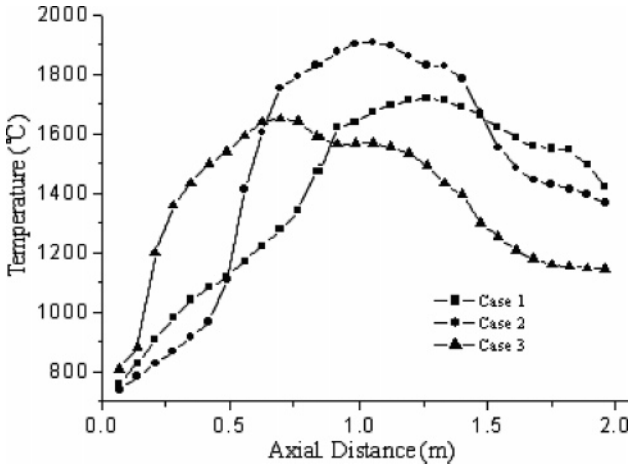

Figure 5. Temperature profiles along the furnace centerline.

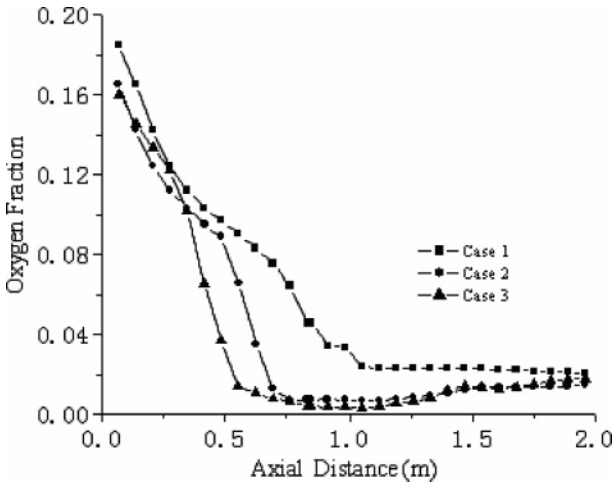

Figure 6. Oxygen fraction profiles along the furnace centerline.

The oxygen fraction profiles were obtained in Figure 6 for three cases. The oxygen fraction distribution for case 1 is relatively even, and the oxygen is sufficient for the full combustion of the pulverized coal in the fuel-rich region. However, for cases 2 and 3, the oxygen concentration in the fuel-rich region is low. Under this condition, a local reducing environment occurs, especially in case 3; the oxygen concentration in the fuel-rich region is the lowest in all cases. This probably prolongs the burnout time or even makes the pulverized coal burn out insufficiently, and the peak temperature decreases correspondingly.

Figure 7 illustrates the concentration distribution of vaporized ash for each case. Significant can be obtained

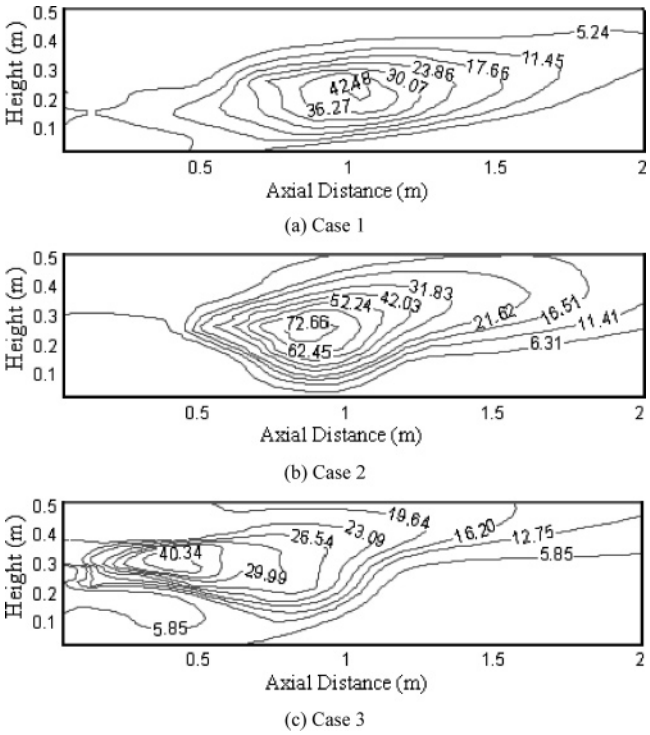

Figure 7. Concentration distribution of vaporized ash for three cases (given in units of mg/m^3).

from the figure that the ash vaporization occurs mostly in the high-temperature region in the furnace, the concentration of vaporized ash reaches the maximum at the peak temperature for each case, and the amount of vaporized ash decreases rapidly with the gas temperature reducing. Furthermore, the peak concentration of vaporized ash is revealed in case 2, its value is obviously higher than that of other two cases, though the oxygen concentration of case 2 and 3 is lower than that of case 1, and the peak concentration for case 3 is slightly lower than that for case 1 because of the influence of temperature distribution. The previously description indicates that the amount of ash vaporization is very sensitive to temperature, and the effect of oxygen concentration on the vaporization is not so obvious compared with the influence of temperature. This is very consistent with the results reported.[9,16,26]

The effect of temperature on ash vaporization can be clearly observed by analyzing individual trajectories. Figures 8 and 9 illustrate the fraction of ash vaporized and particle temperature along low ash vaporization and high ash vaporization trajectories for case 2,

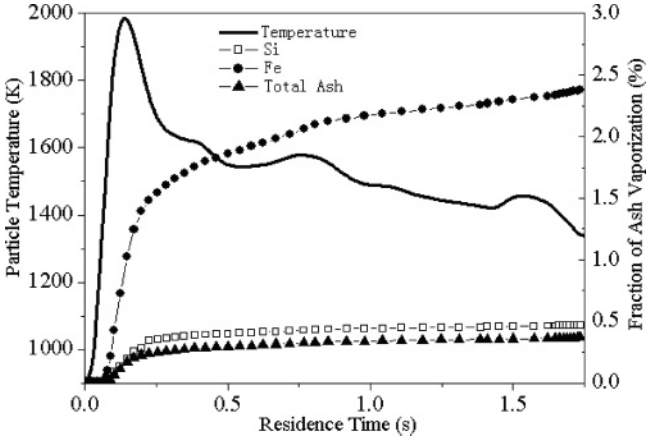

Figure 8. Particle temperature and the cumulative percentage of ash vaporized for low vaporization trajectory (particle size: 100 μm).

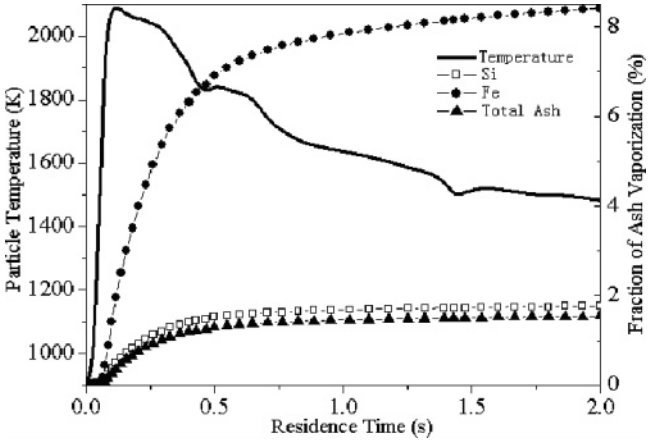

Figure 9. Particle temperature and the cumulative percentage of ash vaporized for high vaporization trajectory (particle size: 100 μm).

respectively; the figures also illustrate the fraction of Si and Fe vaporized. It can be seen in Figure 8 that the particle temperature reaches its peak value of 1980 K at a residence time of approximately 0.13 s, and it is evident that this is where the bulk of the vaporization occurs. But, due to a rapid drop of the particle temperature, the trajectory spends most of its time considerably below 1800 K and thus contributes to the overall vaporized ash by a percentage of 0.37% at the outlet of the furnace. In Figure 9, the particle temperature reaches its peak value of 2090 K at a residence time of approximately 0.15 s and keeps a relatively high value (say, more than 1800 K) until 0.75 s. The slight difference of the particle temperature and residence time in the high-temperature region, experienced by the two trajectories, is enough to cause the ash vaporization fraction to increase markedly during this period. The fraction of ash vaporization of the high ash vaporization trajectory reaches 1.55% at the outlet of the furnace. This further proves the previous conclusion that temperature is the most important influence factor of ash vaporization.

6. Conclusions

To investigate ash vaporization in the coal combustion process and the effects of different combustion conditions, including air staging, on the ash vaporization, a vaporization model is developed and integrated into a CFD code to simulate ash vaporization. The model is validated by a single-particle calculation. The following conclusions can be drawn from the model predictions in a laboratory-scale single-burner furnace.

(1) Air staging has great influence on ash vaporization. Staging changes the distribution of gas temperature and oxygen concentration, as well as the locations of the peak temperature and the high-temperature region in the furnace. The more extreme the staging condition, the lower the overall peak temperature, and hence the lower the amount of ash vaporization.

(2) The effect of temperature on ash vaporization can be clearly observed by analyzing individual vaporization trajectories. The simulation results showed that temperature is the most important influence factor of the ash vaporization compared with other combustion conditions.

Acknowledgment. This work was sponsored by Natural Science Foundation of China (No. 50325621) and the National Key Basic Research and Development Program, the Ministry of Science and Technology of China (2002CB211602).

EF049693L